論文の内容の要旨

ABSTRACT OF DESSERTATION

First-Principles Study toward the Understanding of a Silver Sulfide Atomic Switch

(硫化銀原子スイッチの理解に向けた第一原理研究)

王　中長　(Zhongchang WANG)

1. INTRODUCTION

Most electronic appliances are based on digital electronics, which in essence just require a lot of switches working together in an organized fashion. Recently, much research has been aimed at finding novel switches that can replace conventional silicon-based technology and permit ever smaller and even more powerful electronics. A lot of nanoscale switches have already been fabricated. However, most of the switches involve non-nanoscale components, which makes such switches useful for fundamental researches, but far from potential applications as an actual device.

To solve the problem, Terabe *et al.* proposed a novel atomic switch using mixed ionic conductor Ag_2S.[1] This atomic switch has the advantages of bearing simple structure, stability, reliability and operability, and being easy to transfer to real electronic circuit. In their research, an Ag_2S layer is connected to battery through two metallic leads (at least one is silver). They speculated that Ag atoms are first accumulated at the interface between silver sulfide and a negative silver electrode, and then diffused into the inner part of silver sulfide and finally, a conductive Ag bridge inside the Ag_2S is generated to make the system switch *ON*. Switch *OFF* can be fulfilled through reversing polarity of the applied voltages. Though a lot of intriguing results have already been obtained concerning this switch, its working mechanism has not been well clarified yet. Understanding the mechanism of switching will be vital for controlling and fully exploiting this nanoscale switch as functional electronic components.

The ultimate goal of our study, considering the above situation, is to clarify the switching mechanism of the Ag_2S atomic switch from first principles. To this end, we have examined several aspects of atomic and electronic structures in both bulk Ag_2S and Ag–Ag_2S–Ag heterostructure. Here, we first report results on migration energetics and pathways of an Ag ion in low-temperature Ag_2S. After that, we examine atomic structure, electronic states and electron transport properties of the Ag–Ag_2S (β–phase)–Ag system. Note that hereafter Ag_2S designates the β–phase Ag_2S. Finally, we examine transport property of the systems with excess Ag atoms.

2. SYSTEM INVESTIGATED AND COMPUTATIIONAL DETAILS

In the Ag_2S, the anions (S) forms a distorted body-centered-cubic lattice, while the cations (Ag) are located in sites close to the centers of the octahedral (*O*) and tetrahedral (*T*) sites within the anion sublattice.

We investigated diffusions of Ag ion from a *T* (*O*) site to its neighboring *T* (*O*) vacancy by performing calculations using a 48–atom supercell, adopting the nudge elastic-band (NEB) method in the VASP code.[2] After that, molecular dynamics simulations were carried out using a 96–atom supercell.[2]

As for Ag–Ag_2S–Ag system, our model is shown in Fig. 1. The model can be divided into left semi-infinite electrode, scattering region, and right semi-infinite electrode. The scattering region consists of Ag_2S layers and four or eight surface layers of the left and right electrodes. Two different kinds of interface orientations are considered, and several models within these orientations are constructed, as will be described later.

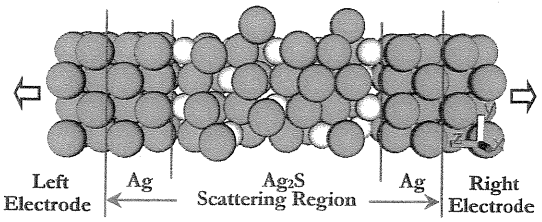

Fig. 1. Schematic illustration of the Ag–Ag_2S–Ag system. The Smaller balls represent S atoms while the larger ones represent Ag atoms.

The electron transport properties of the heterostructure are explored with fully self-consistent nonequilibrium Green's function method implemented in Atomistix ToolKit code.[3] This method has been applied to many systems successfully, but was applied to heterostructures of metal and solid electrolyte for the first time in this study. The local density approximation and the Troullier-Matrins nonlocal pseudopotential are adopted, and the valence electrons are expanded in a numerical atomic-orbital basis set of single zeta plus polarization (SZP).

3. RESULTS AND DISCUSSION

3.1 Migration of Ag Ions in Low-temperature Ag_2S

We investigated four essential migrations of an Ag ion from two types of lattice sites to their nearest-neighbor vacancies of two kinds in low-temperature Ag_2S, namely, from *T* site to *T* vacancy, *T* to *O* vacancy, *O* to *T* vacancy, and *O* to *O* vacancy by the NEB. The calculated diffusion energy barriers of the corresponding four cases are 0.46, 0.22, 0.32, and 0.67 eV, respectively, which are comparable to experimental values of 0.43–0.48 eV.[4] These results suggest that direct diffusions from *T* to *T* and *O* to *O* are not energetically preferable to indirect ones from *T* to *O* and from *O* to *T*, and that indirect *T*–*O*–*T* and *O*–*T*–*O* migrations are more likely than direct ones, *T*–*T* and *O*–*O*.

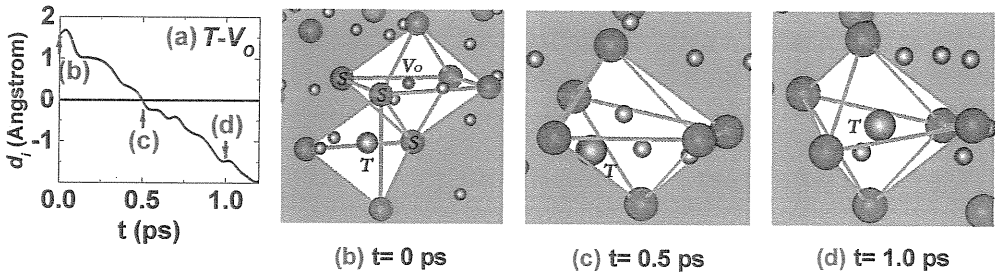

Fig. 2. (a) Time evolution of distance d_i between the focused Ag ion and the triangle formed by three S ions for migration from *T* to *O* vacancy at T = 700K. The evolution of the diffusion trajectory at (b) t=0.0 ps; (c) t=0.5 ps; and (d) t=1.0 ps. The S atoms are all de noted with "S", and the focused mobile Ag atom and the *O* vacancy are marked with 'T' and 'V_O', respectively. For clarity, the tetrah edron and octahedron constituted by S ions are connected with lines.

Figure 2 illustrates the evolution of trajectory of a focused Ag ion migrating from a *T* to its nearest-

neighbor O vacancy in Ag_2S at 700K calculated by the MD. We observed from Fig. 2(b) to Fig. 2(d) that a *T* Ag migrates directly from its original *T* site to its neighbor *O* vacancy through a triangle constructed by three S ions, as denoted in Fig. 2(b). The entire evolution trajectories for an Ag ion migrating from an *O* to its nearest-neighbor *T* vacancy are analogous to those migrating from *T* to its nearest-neighbor *O* vacancy, which are not shown here. These supports the results obtained from the NEB calculation, that is, the preferential migration of Ag ions between nonequivalent sites.

3.2 Atomic and Electronic Transport Properties of Ag–Ag_2S–Ag

Based on the experimentally observed orientation relationships of $(0\text{-}12)_{Ag_2S}//(001)_{Ag}$ and $[100]_{Ag_2S}//[100]_{Ag}$,[5] we constructed three models of the interface structure, where S atoms in the Ag_2S layer proximal to the interface are located on the On-top, Bridge, and Hollow sites of the outmost layer of Ag electrode, respectively. Our calculations show that the *Bridge* case is the most stable one , irrespective of the structural relaxation and applied bias voltages. The Ag_2S lattice constant is elongated by 15.2% along x direction and compressed by 7.1% along y direction.

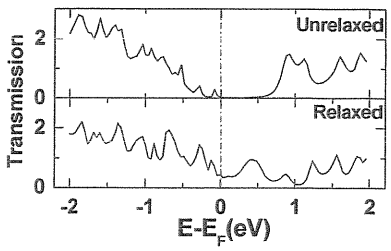

Fig. 3. Transmission spectra for the Bridge case without and with structural relaxation under 0V.

The transmission spectra for structures of the *Bridge* case with and without relaxation are shown in Fig. 3. The transmission coefficient at E_F increases from 0.04 before structural relaxation to 0.455 after relaxation, which shows the opening of a conduction channel in the relaxed structure. Investigation into its atomic arrangement reveals that a zigzag Ag atomic chain is formed in the Ag_2S, whose atomic configuration is illustrated in Fig. 4. The neighboring Ag–Ag distances along the chain range from 2.84Å to 3.07Å (see numbers in Fig. 4), which are very close to the nearest neighbor distance in Ag bulk, 2.89Å, but deviate severely from Ag–Ag separation in the Ag_2S bulk, 3.08–3.74Å.[6]

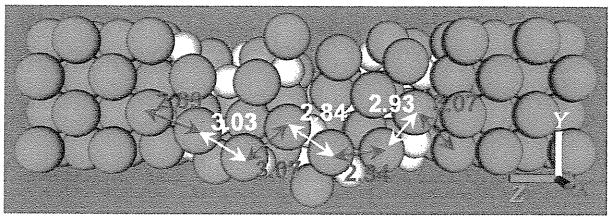

Fig. 4. Atomic arrangement of the relaxed structure of the Bridge case under 0V. The numbers denote the neighboring Ag-Ag distances along the chain in the Ag_2S.

We also investigated electronic and electric properties of the system under applied bias voltages. First, we calculated currents (*I*) under voltages (*V*) ranged from −3.0V to 3.0V using the relaxed *Bridge* structure. The *I*–*V* curve is nearly linear, showing metallic nature of this system, which can be explained by the formation of the zigzag atomic chain. Next, we examined how the applied bias voltages drop along the Ag chain plane. Figure 5 illustrates the difference of the effective potential in the plane including the Ag chain between the case where the bias voltage of 0.5V is applied and the case of 0.0V, for both unrelaxed and relaxed *Bridge* cases. One can see that intensive voltage drop takes place mainly around the negative bias end of the interface region for both cases, which suggests that changes in the Ag_2S

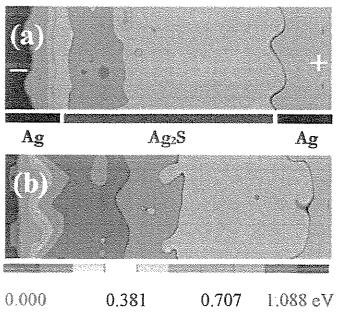

Fig. 5. Difference of effective potential along the Ag chain plane by an applied bias voltage of 0.5V for (a) unrelaxed *Bridge* case, and (b) relaxed *Bridge* case.

layer by applying bias voltage should commence from this area.

3.3 Toward the Understanding of the Silver Sulfide Atomic Switch

In view of the large mismatch in the above model, here, we construct a new model having the orientation relationships of $(001)_{Ag}$ //$(010)_{Ag_2S}$ and $[010]_{Ag}$//$[100]_{Ag_2S}$ instead. In this model, S atoms in the Ag_2S layer proximal to the interface are located at the bridge sites of the outmost layer of Ag electrode. We have confirmed that this model has lower total energy than another possible model with the same orientation relationships. Compared with the previous model, this one has the advantage of smaller lattice mismatch despite relatively small sizes. The Ag_2S lattice constant is elongated by 3.75% along x direction and contracted by 3.56% along y direction to match the Ag electrodes.

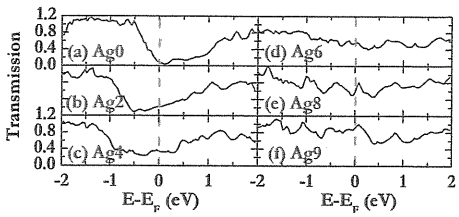

Fig. 6. Transmission spectra for the Bridge cases with excess Ag atoms under 0V.

The transmission coefficient at E_F increases slightly from 0.03 before structural relaxation to 0.09 after relaxation, which shows no opening of conduction channel in the relaxed structure in contrast with the model examined in the previous section. Then, nine excess Ag atoms were inserted into the Ag_2S in turn from the right electrode side. The transmission coefficient at E_F increases to 0.215, 0.358, 0.561, and 0.575 through introduction of two, four, six, and eight excess Ag atoms. Finally, it enhances sharply to 0.909 by introducing nine excess Ag. The change of transmission spectra with the insertions is illustrated in Fig. 6, where we present six representative cases. The valley around E_F in Fig. 6(a) disappears after the insertion of nine excess Ag, which means the system changes its nature from semiconducting to metallic.

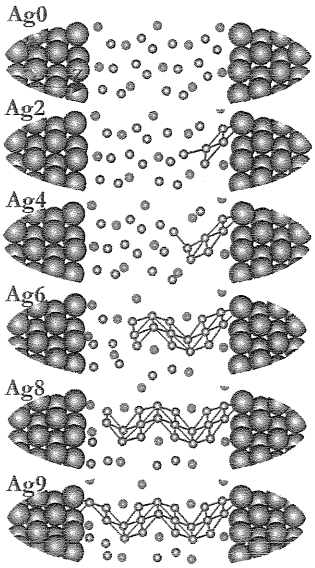

Fig. 7. Simulated formation of a conductive Ag bridge inside the Ag_2S with insertion of excess Ag.

Investigation into atomic configurations of the systems reveals that a conductive Ag bridge is generated gradually as excess Ag are introduced, and finally bridged over the entire Ag_2S when nine excess Ag are inserted, as shown in Fig. 7. The most interesting feature seen in this figure is that the atomic arrangement of the bridge is quite similar to the close-packed Ag (111) faces that have the lowest energy in Ag bulk. As shown from Fig. 8, the neighboring Ag–Ag distances in the face vary from 2.76 Å to 2.99Å (see numbers between Ag atoms in Fig. 8), which are very close to the nearest neighbor distance in (111) face of Ag bulk, 2.89Å, but deviate severely from Ag–Ag separation in the Ag_2S bulk, 3.08–3.74Å. In addition, analysis of Mulliken population shows that the electron loss of respective Ag atoms in the (111) face is smaller than that in Ag_2S bulk, −0.13, but near the value of Ag bulk, 0, for some of Ag atoms (see numbers on each atoms in Fig. 8). This means that Ag atoms along the bridge exhibit more nature of metal Ag than that of Ag in the Ag_2S bulk.

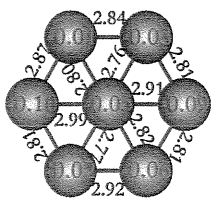

Fig. 8. Atomic configuration of one of Ag (111) faces.

4. CONCLUSIONS

We have performed first-principles calculations toward the understanding of the switching mechanism of the Ag_2S atomic switch. First, we investigated migration pathways and estimated corresponding activation energy barriers in the low-temperature Ag_2S. The calculated energy barriers for the four essential migrations are between 0.21 to 0.67 eV, which are comparable to the experimental values. Migrations between the nearest equivalent positions are not energetically preferable to nonequivalent ones.

Then, we examined electron transport and structural properties of the Ag–Ag_2S–Ag heterostructure. We find that an Ag atomic conductance channel in the Ag_2S is generated after structure optimization, resulting in large enhancement of transmission and the metallic behavior of the heterostructure.

Finally, we find, through insertion of excess Ag atoms, that a conductive Ag bridge is generated inside the Ag_2S, whose structure is similar to that of Ag (111), leading to sharp enhancement of transmission when connected to the two electrodes.

REFERENCE

1. K. Terabe, T. Hasegawa, T. Nakayama, and M. Aono, *Nature* **433**, 47 (2005).
2. Z. C. Wang, Tingkun Gu, T. Kadohira, T. Tada, and S. Watanabe, *The Jouranl of Chemical Physics*, In Press.
3. M. Brandbyge, J. Mozos, P.Ordjon, J. Taylor, and K. Stokbro, *Phys. Rev. B* **65**, 165401 (2002).
4. R. L. Allen and W. J. Moore, *J. Phys. Chem.* **63**, 223 (1959).
5. Z. C. Wang, T. Kadohira, T. Tada, and S. Watanabe, *Nano Lett.* **7**, 2688 (2007).
6. R. Sadanaga and S. Sueno, *Mineral. J.* **5**, 124 (1967).